The International Archives of the Photogrammetry, Remote Sensing and Spatial Information Sciences, Volume XLIX-B3-2026
XXV ISPRS Congress 2026 "From Imagery to Understanding", Commission III, 4–11 July 2026, Toronto, Canada

Integrating MTInSAR and Geoscientific Data for Subsurface Deformation Monitoring in the Epe Cavern Field, Germany

Chia-Hsiang Yang[1], Marcin Pawlik[2], Tobias Rudolph[2], Sebastian Teuwsen[1], Carsten Stemmler[1], Peter Goerke-Mallet[2], Andreas Müterthies[1]

[1] EFTAS Remote Sensing Transfer of Technology, Münster, Germany - chia-hsiang.yang@eftas.com
[2] Research Centre of Post-Mining, Technische Hochschule Georg Agricola, Bochum, Germany - tobias.rudolph@thga.de

Keywords: MTInSAR, Subsurface Deformation, Data Integration, Cavern Storage, Geohazard Assessment, Geospatial Monitoring.

Abstract

Subsurface gas storage in salt caverns induces spatially variable ground deformation that requires continuous and large-scale monitoring. This study presents an integrated analysis of multi-temporal InSAR (MTInSAR) and geoscientific data for the Epe cavern field in Germany, based on results from the Forschungskooperation Epe and REWE projects. Sentinel-1 data were processed using an Enhanced Small Baseline Subset (E-SBAS) approach to derive deformation time series from 2015 to 2025. Line-of-sight measurements were decomposed into vertical and east–west components to enable physically meaningful interpretation. A clustering-based strategy was applied to classify deformation patterns and identify spatially coherent deformation regimes. The results reveal a persistent bowl-shaped subsidence structure combined with systematic horizontal convergence toward the deformation centre. Long-term analysis confirms stable spatial patterns with progressive deformation accumulation. The integration of MTInSAR with geoscientific context enhances the interpretation of subsurface processes and provides a robust framework for operational-scale deformation monitoring and risk assessment.

1. Introduction

Subsurface gas storage in salt caverns can cause slow and spatially variable ground deformation that requires continuous, large-scale monitoring for safe and sustainable operation. The Epe research cooperation (Forschungskooperation Epe, 2015–2025), jointly conducted by THGA and EFTAS, established an integrated Earth Observation framework combining Sentinel-1 multi-temporal InSAR (MTInSAR) analyses with geological, hydrological, and geotechnical datasets to investigate deformation dynamics in the Epe cavern field in western Germany (Rudolph et al., 2024, 2026).

In parallel, the research cooperation "Radarfernerkundung – Epe – West-East (REWE)" focused on the joint analysis of vertical and horizontal ground movements using SBAS-based MTInSAR, clustering approaches, and multi-criteria analysis. This enabled the identification of spatial deformation patterns and their relation to subsurface processes and operational conditions.

The workflow applies MTInSAR processing based on the Small Baseline Subset (SBAS) method (Lanari et al., 2004; Pepe et al., 2011), enabling the derivation of long-term deformation time series over large areas. The combined outcomes of these first-phase projects provide the methodological and analytical basis for the present study.

Within this context, this study presents the integration of MTInSAR-derived deformation products with geoscientific data to analyse long-term ground movement patterns and their spatial variability in the Epe cavern field. Building on these results, follow-up initiatives aim to further extend the framework toward enhanced data integration, process understanding, and application-oriented geomonitoring.

The remainder of this paper is organized as follows. Section 2 introduces the MTInSAR processing methodology, including deformation decomposition and clustering-based analysis. Section 3 presents the experimental results for vertical and horizontal deformation, as well as their joint interpretation and long-term evolution. Section 4 provides a discussion of the deformation mechanisms and the added value of integrating geoscientific data. Finally, Section 5 concludes the paper and outlines future research directions.

2. Data and Methods

2.1 Sentinel-1 MTInSAR Processing

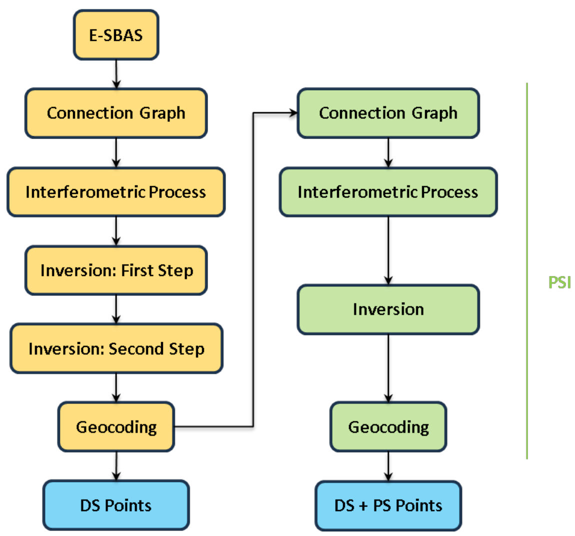

Figure 1. SARscape Enhanced SBAS (E-SBAS) processing workflow used for the MTInSAR time-series analysis in this study.

MTInSAR processing was carried out using the Enhanced SBAS (E-SBAS) workflow implemented in SARscape (Lanari et al., 2004; Pepe et al., 2011). The processing chain is summarized in

Figure 1 and was used to generate deformation velocities and deformation time series for subsequent component decomposition (Section 2.2) and geodata integration (Section 2.3).

The workflow starts with the construction of an interferometric connection graph, which defines the interferogram network used for time-series estimation. Based on this graph, an interferometric processing stage generates differential interferograms, including co-registration, removal of topographic phase using an external DEM, and phase filtering.

Time-series estimation is performed by a two-stage inversion (Inversion: First Step and Inversion: Second Step). The first inversion step provides an initial solution and identifies reliable measurement points dominated by DS-points. The second inversion step refines the deformation estimates by exploiting network redundancy and improving phase consistency across the stack. The final deformation products are then geocoded to map coordinates for spatial analysis.

SARscape also provides a PSI-oriented alternative branch (Ferretti et al., 2011; Goel and Adam, 2014), where PS-points can be combined with DS points to increase point density in urban environments. In this study, E-SBAS was selected as the primary MTInSAR strategy to ensure robust deformation retrieval over the mixed land-cover conditions of the Epe cavern field.

2.2 Deformation Decomposition

MTInSAR processing provides deformation measurements along the radar line-of-sight (LOS) direction for each satellite acquisition geometry. Because LOS measurements represent a projection of the true three-dimensional deformation vector onto the viewing direction of the sensor, they do not directly correspond to vertical or horizontal motion. To improve interpretability for infrastructure monitoring, LOS observations from ascending and descending Sentinel-1 tracks were combined to estimate vertical and east–west deformation components.

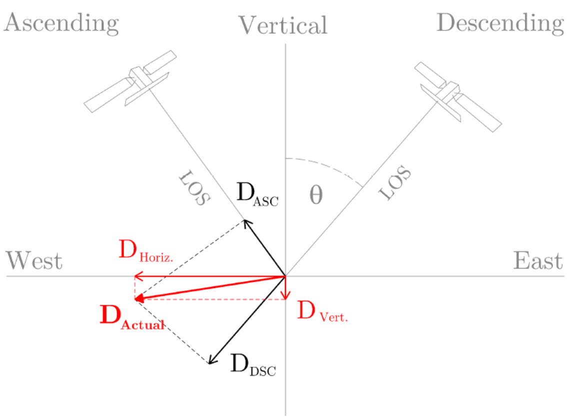

Figure 2. Conceptual geometry of deformation decomposition using ascending and descending LOS observations. The actual ground displacement vector D_{Actual} is projected onto the radar line-of-sight directions D_{ASC} and D_{DSC}. By combining both viewing geometries, vertical $D_{Vert.}$ and east–west horizontal $D_{Horiz.}$ deformation components can be estimated.

The geometric principle of the decomposition is illustrated in Figure 2. Ascending and descending satellites observe the ground from opposite viewing directions, producing two independent LOS measurements D_{ASC} and D_{DSC}. The actual ground displacement vector D_{Actual} can be conceptually separated into a vertical component $D_{Vert.}$ and a horizontal component in east–west direction $D_{Horiz.}$. By combining the two LOS observations, the vertical motion and the east–west motion can be retrieved.

Due to the near-polar orbit configuration of Sentinel-1, sensitivity to north–south deformation is limited. Therefore, the decomposition assumes that north–south motion is negligible compared to vertical and east–west components at the scale of the Epe cavern field. This assumption is commonly adopted in similar deformation studies and is considered reasonable given the geological setting and expected deformation kinematics.

To ensure numerical stability, ascending and descending deformation fields were resampled onto a consistent spatial grid before decomposition. The resulting products include:

- Vertical deformation velocity and cumulative deformation time series.
- East–west deformation velocity and cumulative deformation time series.

These component-based deformation maps provide a more physically meaningful representation of subsidence bowl geometry and lateral motion patterns than LOS measurements alone and form the basis for the integrated geodata analysis presented in Section 2.3.

2.3 Clustering Strategy

To systematically characterize spatial and temporal variability of ground deformation, a clustering-based analysis strategy was implemented. The purpose of this approach is to group areas exhibiting similar deformation dynamics into homogeneous classes and thereby enable structured comparison of deformation regimes across the study area.

All MTInSAR-derived deformation products were processed in a GIS-based analytical environment using ArcGIS Pro and Python-supported workflows. Deformation time-series information was first organized in a Space-Time Cube, where each spatial unit is represented by its temporal deformation evolution. This representation enables consistent handling of multi-year deformation records and provides a foundation for spatiotemporal statistical analysis.

K-means clustering (Everitt et al., 2011) was then applied to classify deformation behaviour. The k-means algorithm partitions the dataset into a predefined number of clusters by minimizing within-cluster variance while maximizing separation between clusters. For vertical deformation, clustering features were derived from cumulative subsidence values and temporal trend characteristics. The number of clusters was selected to capture dominant deformation intensity levels while preserving interpretability of deformation regimes.

The clustering was performed exclusively on deformation-derived metrics, while contextual datasets such as soil or geological information were intentionally excluded from the clustering variables. This ensures that the classification reflects intrinsic deformation behaviour without bias from explanatory factors. The applied clustering approach follows and extends previous work on k-means-based classification of SBAS-InSAR deformation fields in the Epe cavern area, where clustering was demonstrated as an effective method for identifying coherent deformation regimes in both vertical and horizontal components. The resulting clusters provide a compact representation of deformation patterns and form the methodological basis for the

https://doi.org/10.5194/isprs-archives-XLIX-B3-2026-537-2026 | © Author(s) 2026. CC BY 4.0 License.

spatial classification maps and cluster-based time-series analysis presented in Section 3.

3. Experiments and Results

3.1 Vertical Ground Movement 2015 - 2021

The vertical deformation field derived from Sentinel-1 MTInSAR for 2015–2021 reveals a coherent subsidence bowl across the Epe cavern field (Figure 3). Subsidence is concentrated around the cavern cluster and gradually decreases toward the periphery, forming a spatial pattern consistent with the superposition of deformation contributions from multiple caverns rather than isolated single-cavern signatures. The velocity scale in Figure 3 indicates predominantly negative vertical deformation rates within the central zone, while surrounding areas show lower magnitudes and smoother gradients.

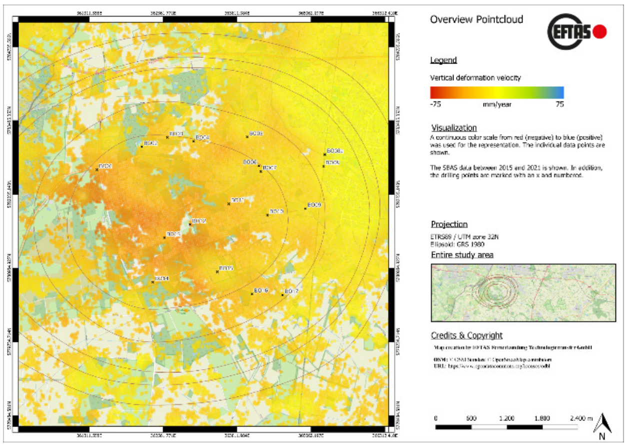

Figure 3. Vertical deformation velocity map derived from Sentinel-1 MTInSAR for 2015–2021, showing a bowl-shaped subsidence structure across the Epe cavern field. The deformation is displayed as a point cloud, with selected reference points (B001–B017) indicated for interpretation and time-series analysis.

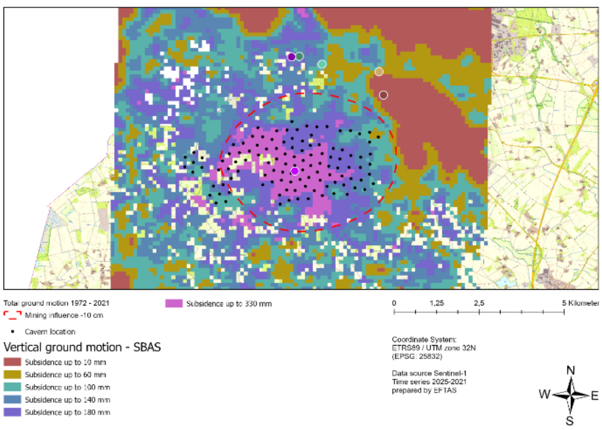

Figure 4. Vertical cumulative subsidence classification map.

The map is represented as a dense point cloud of MTInSAR measurement points, enabling detailed visualization of spatial variability. In addition, selected reference locations (B001–B017) are highlighted for consistent reporting and subsequent comparison with time-series behaviour. The spatial structure of the subsidence field is broadly circular to elliptical, suggesting a large-scale deformation response driven by subsurface convergence processes, with local deviations reflecting heterogeneity in the deformation expression across the storage area. Overall, the vertical deformation pattern demonstrates that Sentinel-1 MTInSAR provides spatially continuous information on subsidence dynamics over the full monitoring area, which forms the basis for the subsequent east–west analysis (Section 3.2) and the integrated interpretation (Section 3.3).

To enable a systematic interpretation of spatial variability, a vertical clustering approach was applied to classify cumulative vertical deformation into six intensity classes. The resulting classification map is presented in Figure 4. The spatial distribution of clusters indicates that subsidence is primarily concentrated in the vicinity of actively used caverns; however, measurable deformation extends beyond the immediate cavern field, demonstrating that the surface response reflects the collective deformation behaviour of the storage complex.

The six vertical deformation classes represent increasing cumulative subsidence intensity, and their temporal evolution is summarized in Figure 5 using cluster-based time series (solid line: representative pixel; dotted line: cluster mean):

- Class 1 (red), Stable reference zone (~ −10 mm). Minimal vertical movement. The time series remains nearly stable (Figure 5), supporting its use as a reference area for comparison.
- Class 2 (brown), Moderate subsidence (~ −60 mm). A broad transitional ring around more active zones. Time series show a gentle but persistent negative trend, indicating slow continuous subsidence.
- Class 3 (green–blue), Moderate–persistent subsidence (~ −100 mm). A wider boundary around the central deformation core with steady negative trends and attenuated magnitudes compared to inner zones.
- Class 4 (blue), Pronounced subsidence (~ −140 mm). Persistent downward trends forming part of the outer high-intensity deformation belt.
- Class 5 (violet), Strong subsidence (~ −170 mm). Zones closer to the cavern cluster showing substantial cumulative deformation and sustained downward motion.
- Class 6 (pink), Maximum subsidence (~ −280 mm). The highest deformation magnitudes, spatially coinciding with the central cavern complex (black dots in Figure 4). The time series exhibits the steepest cumulative trend (Figure 5), indicating localized but intense vertical ground movement.

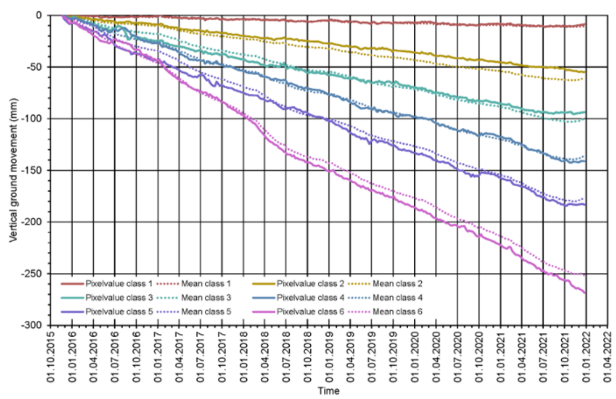

Figure 5. Cluster-based vertical time-series evolution.

3.2 East-West Ground Movement 2015 - 2021

The east–west deformation component derived from the MTInSAR decomposition reveals a spatially coherent pattern of opposing horizontal ground motion across the Epe cavern field. The spatial classification of horizontal movement directions is shown in Figure 6, where areas are grouped into three categories: eastward movement, westward movement, and stable zones.

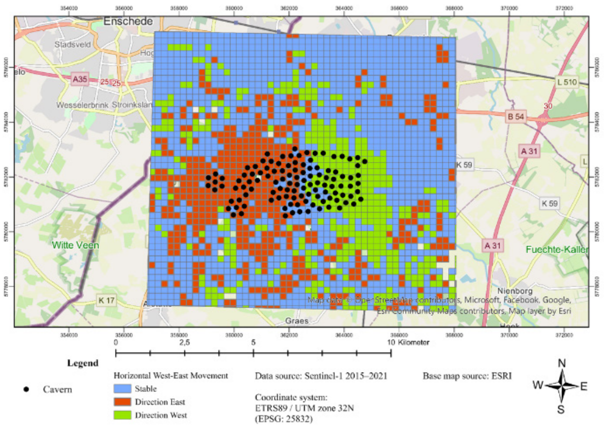

Figure 6. East–west ground movement classification derived from Sentinel-1 MTInSAR for the period 2015–2021. Areas are categorized into eastward movement, westward movement, and stable zones. The spatial pattern reveals opposing horizontal displacement directions on either side of the central cavern cluster (black dots), consistent with inward convergence toward the subsidence core.

The deformation pattern exhibits a structured convergence behaviour toward the central subsidence area identified in Section 3.1. The western sector of the cavern field predominantly shows eastward-directed movement, while the eastern sector exhibits westward-directed movement. Between these two domains, a narrow transition zone of near-stable behaviour is observed. This spatial configuration is consistent with kinematic expectations for a subsidence bowl, where horizontal motion vectors tend to point toward the zone of maximum vertical deformation.

The alignment of horizontal movement with cavern distribution is evident in Figure 6, where the strongest opposing directions spatially coincide with the main cavern cluster. The pattern indicates that horizontal deformation is not randomly distributed but reflects systematic stress redistribution within the storage complex.

The temporal evolution of representative pixels and corresponding cluster means is shown in Figure 7. The red curves (eastward movement) display a steadily increasing positive displacement trend over the observation period, reaching cumulative values of approximately +20 to +25 mm. Conversely, the blue curves (westward movement) exhibit a persistent negative trend, reaching cumulative values of approximately −20 to −30 mm by 2021. The stable cluster (green curves) remains close to zero throughout the time series, confirming its classification as a transitional or low-dynamic zone.

The consistency between individual pixel trajectories (solid lines) and cluster means (dotted lines) indicates that the horizontal deformation signal is coherent within each class and not dominated by isolated outliers. The gradual and sustained character of the displacement trends suggests that horizontal motion is governed primarily by long-term subsurface convergence processes, with potential modulation by operational cycles.

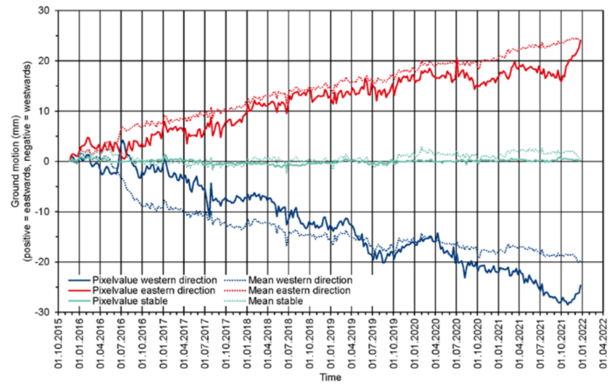

Figure 7. Cluster-based time-series evolution of east–west ground movement (2015–2021). Solid lines represent representative pixel trajectories within each movement class, while dotted lines indicate the corresponding cluster means. Positive values denote eastward motion and negative values denote westward motion. The results demonstrate persistent and coherent horizontal displacement trends over the observation period.

Overall, the east–west deformation results complement the vertical subsidence analysis and confirm a mechanically consistent deformation field characterized by inward horizontal movement toward the central subsidence core. The structured opposition of horizontal directions further supports interpretation of a large-scale deformation bowl rather than isolated localized disturbances.

3.3 Joint Analysis on Ground Movement 2015 - 2021

To obtain an integrated understanding of the deformation regime above the Epe cavern field, vertical and east–west deformation components were jointly analysed. The combined deformation behaviour of representative positions is illustrated in Figure 8, where cumulative vertical displacement is plotted against cumulative horizontal displacement for selected locations within the cavern field.

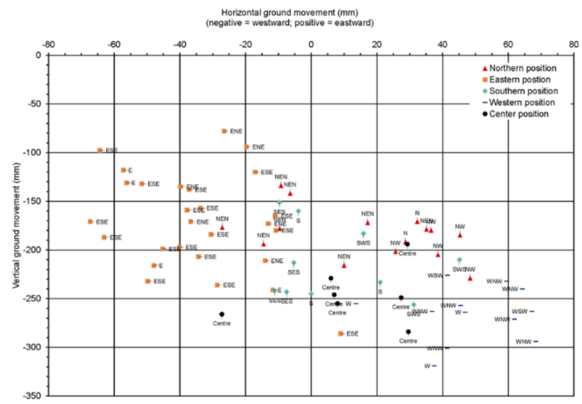

Figure 8. Joint representation of cumulative vertical and east–west ground movement (2015–2021) for selected positions within the Epe cavern field. Horizontal displacement (positive = eastward; negative = westward) is plotted against vertical displacement. The structured distribution of points illustrates inward horizontal convergence toward the subsidence core combined with increasing vertical deformation toward the centre.

The joint representation reveals a structured distribution of deformation vectors. Points located in the western sector of the

https://doi.org/10.5194/isprs-archives-XLIX-B3-2026-537-2026 | © Author(s) 2026. CC BY 4.0 License.

cavern field predominantly exhibit negative horizontal displacement (westward motion) combined with strong vertical subsidence. Conversely, points in the eastern sector show positive horizontal displacement (eastward motion), also accompanied by significant vertical subsidence. Central positions display the largest vertical deformation magnitudes while showing relatively small horizontal displacement, indicating that vertical convergence dominates near the subsidence core.

This systematic arrangement confirms the bowl-shaped deformation geometry inferred from Sections 3.1 and 3.2. Horizontal motion is directed toward the central subsidence area from both sides, while vertical deformation intensifies toward the centre. The spatial differentiation between northern, southern, eastern, and western positions further indicates that the deformation field is not isotropic but exhibits directional variability consistent with stress redistribution within the cavern system.

The clustering-based time-series analysis presented in previous sections is supported by this joint evaluation. Positions classified as stable or transitional show limited horizontal displacement and moderate vertical subsidence, whereas highly active deformation zones combine strong vertical movement with systematic horizontal convergence.

The joint analysis therefore confirms that the deformation field is mechanically coherent and reflects a coupled vertical–horizontal response driven by subsurface convergence processes. The observed deformation vectors are consistent with a large-scale deformation bowl influenced by the spatial configuration of caverns and long-term salt creep dynamics.

3.4 Long-Term Monitoring 2015 - 2025

To assess the temporal evolution of ground deformation beyond the initial analysis period (2015–2021), the MTInSAR time series was extended to October 2025. This extended observation period enables a more comprehensive evaluation of long-term deformation trends and their spatial persistence across the Epe cavern field.

The vertical deformation field derived from Sentinel-1 MTInSAR is shown in Figure 9. The results confirm the continuation of the previously identified bowl-shaped subsidence structure, with the most pronounced deformation located in the central cavern area. Compared to the earlier period, the spatial pattern remains largely stable, indicating a persistent deformation regime controlled by subsurface processes. However, an increase in deformation magnitude can be observed in localized zones, particularly in the central and southwestern parts of the study area, where cumulative subsidence continues to intensify. The outer zones exhibit relatively stable conditions, with only minor deformation signals, suggesting a clear spatial gradient from the centre towards the periphery.

The horizontal (east–west) deformation field for the same period is presented in Figure 10. Similar to the earlier results (Section 3.2), a distinct pattern of opposing lateral movements is observed. The central and eastern parts of the cavern field show dominant eastward motion, while the western areas exhibit westward displacement. This opposing behaviour remains consistent over the extended time period, indicating a stable and systematic deformation mechanism rather than short-term fluctuations. The spatial distribution of horizontal deformation aligns well with the vertical subsidence pattern, reinforcing the interpretation of coupled deformation processes.

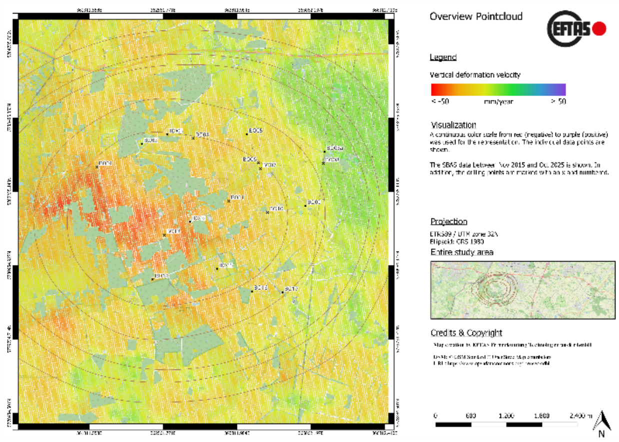

Figure 9. Vertical deformation velocity map derived from Sentinel-1 MTInSAR for the extended period 2015–2025, showing the persistent bowl-shaped subsidence pattern across the Epe cavern field and increased deformation magnitude in the central cavern area.

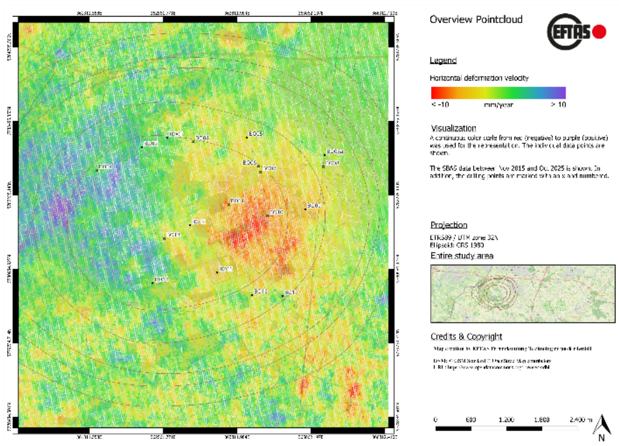

Figure 10. Horizontal east–west deformation velocity field derived from Sentinel-1 MTInSAR for the period 2015–2025, illustrating consistent opposing lateral movements with eastward displacement in the central–eastern zones and westward displacement in the western areas.

The comparison between the 2015–2021 and 2015–2025 results highlight the temporal consistency of the deformation signals. While the overall spatial patterns remain stable, the extended time series reveals a progressive accumulation of deformation, particularly in areas directly associated with cavern operations. This demonstrates the importance of long-term MTInSAR monitoring for capturing both persistent trends and gradual changes in deformation dynamics.

Overall, the extended analysis confirms that the deformation behaviour in the Epe cavern field is not transient but represents a long-term, spatially coherent process. The combination of vertical and horizontal deformation observations over a decade provides a robust basis for interpreting subsurface mechanisms and supports the integration of MTInSAR results into operational monitoring frameworks.

4. Discussion

The integration of vertical and horizontal MTInSAR-derived deformation fields provides a comprehensive understanding of the ground deformation dynamics in the Epe cavern field. The results demonstrate a high degree of spatial and temporal consistency across the observation period from 2015 to 2025, indicating that the detected deformation patterns are governed by persistent subsurface processes rather than short-term or random effects.

The vertical deformation analysis reveals a pronounced bowl-shaped subsidence structure centred on the main cavern area, with deformation magnitudes decreasing radially towards the periphery. This spatial configuration is characteristic of large-scale subsurface volume changes and is consistent with the expected behaviour of salt cavern systems under operational conditions. The clustering results further highlight the heterogeneity of deformation intensity, distinguishing between stable outer zones and highly active central areas directly associated with cavern locations.

The horizontal deformation results complement this interpretation by showing systematic, opposing east–west movements. The spatial alignment between vertical subsidence and horizontal displacement patterns suggests a coupled deformation mechanism, where vertical compaction is accompanied by lateral mass redistribution. This behaviour can be attributed to pressure variations within the caverns and the viscoplastic response of the surrounding salt rock, leading to gradual deformation over time.

The joint analysis of vertical and horizontal components confirms that the deformation field is not isotropic but exhibits directional characteristics linked to subsurface structures and operational influences. The observed deformation gradients and directional trends indicate that the mechanical response of the subsurface is spatially variable, likely influenced by cavern geometry, depth, and operational history. This highlights the importance of analysing multi-dimensional deformation components rather than relying solely on line-of-sight measurements.

The extension of the time series to 2025 demonstrates that the deformation processes are continuous and cumulative. While the overall spatial patterns remain stable, the increasing deformation magnitude in specific zones underscores the need for long-term monitoring to capture progressive changes. The consistency of the results across different time periods also confirms the reliability of Sentinel-1 MTInSAR for operational-scale deformation monitoring.

Finally, the integration of MTInSAR results with geoscientific information enhances the interpretability of the observed deformation patterns. By linking surface deformation signals with subsurface processes, the approach supports a more comprehensive assessment of ground stability and provides valuable insights for the safe and sustainable operation of underground storage systems. Overall, the study demonstrates that combining multi-temporal SAR analysis with geoscientific context enables a robust and scalable framework for subsurface deformation monitoring.

5. Conclusions and Future Work

This study demonstrates that the integration of MTInSAR with geoscientific datasets provides a robust framework for analysing long-term ground deformation in complex subsurface environments such as the Epe cavern field. By combining vertical and horizontal deformation components with clustering-based pattern analysis, spatially coherent deformation zones can be identified and linked to underlying subsurface processes.

The results are based on the first-phase research activities of the Forschungskooperation Epe and REWE projects, which established a consistent methodological framework for large-scale deformation monitoring using Sentinel-1 data in combination with integrated geodata analysis. The presented results highlight the capability of satellite-based monitoring to capture both spatial variability and temporal evolution of ground movement over extended time periods.

At the same time, the findings indicate that a comprehensive interpretation of deformation patterns requires a deeper integration of additional data sources, including operational, geological, hydrological, and environmental information. In particular, the interaction between anthropogenic influences and natural processes remains a key challenge for the interpretation of observed deformation signals.

Building on these results, ongoing follow-up initiatives aim to further extend the analytical framework. The project focuses on integrating cavern-specific operational data, improving validation through in-situ measurements, and refining clustering-based approaches for deformation pattern analysis. In parallel, we plan to further develop the integrated geomonitoring framework by incorporating additional geoscientific and environmental datasets, enabling a more comprehensive understanding of coupled surface–subsurface processes.

Future work will therefore focus on improving process understanding, strengthening interdisciplinary data integration, and developing scalable monitoring approaches that support risk assessment and decision-making for infrastructure and environmental management.

6. Acknowledgement

The authors acknowledge the use of Sentinel-1 data provided by the European Union's Copernicus Programme. The study is based on the results of the Forschungskooperation Epe (2015–2025) and the research cooperation REWE, jointly carried out by EFTAS Fernerkundung Technologietransfer GmbH and the Technische Hochschule Georg Agricola (THGA).

The authors gratefully acknowledge the financial and technical support provided by Uniper Energy Storage GmbH within the framework of both research cooperation projects.

References

Everitt, B.S., Landau, S., Leese, M., Stahl, D., 2011. Cluster Analysis, 5th Edition, Cluster Analysis, 5th Edition. wiley.

Ferretti, A., Fumagalli, A., Novali, F., Prati, C., Rocca, F., Rucci, A., 2011. A New Algorithm for Processing Interferometric Data-Stacks: SqueeSAR. IEEE Trans. Geosci. Remote Sens., 49(9), 3460–3470.

Goel, K., Adam, N., 2014. A Distributed Scatterer Interferometry Approach for Precision Monitoring of Known Surface Deformation Phenomena. IEEE Trans. Geosci. Remote Sens., 52(9), 5454–5468.

Lanari, R., Mora, O., Manunta, M., Mallorqui, J.J., Berardino, P., Sansosti, E., 2004. A Small-baseline Approach for Investigating Deformations on Full-resolution Differential SAR Interferograms. IEEE Trans. Geosci. Remote Sens., 42(7), 1377–1386.

Pepe, A., Euillades, L.D., Manunta, M., Lanari, R., 2011. New Advances of The Extended Minimum Cost Flow Phase Unwrapping Algorithm for SBAS-DInSAR Analysis at Full Spatial Resolution. IEEE Trans. Geosci. Remote Sens., 49(10), 4062–4079.

Rudolph, T., Goerke-Mallet, P., Homölle, A., Müterthies, A., Perrevort, H., Teuwsen, S., & Yang, C. H. (2024). Participatory Geomonitoring for Future Mining—Resilience Management in the Cavern Storage Epe (Germany). Mining 2024, Vol. 4, Pages 230-247, 4(2), 230–247. https://doi.org/10.3390/MINING4020014

Rudolph, T., Pawlik, M. P., Yang, C.-H., Przyrowski, R., Müterthies, A., Teuwsen, S., & Hegemann, M. (2026). Application of K-Means Clustering for the Analysis of Horizontal and Vertical SBAS-InSAR Ground Movement Data Above Europe’s Largest Underground Cavern Gas Storage Gronau-Epe. Mining 2026, Vol. 6, 6(1), 23. https://doi.org/10.3390/mining6010023